Visual Coverage Maintenance for Quadcopters Using Nonsmooth Barrier Functions

Riku Funada[1], María Santos[2], Takuma Gencho[3], Junya Yamauchi[3], Masayuki Fujita[3], and Magnus Egerstedt[2]

***Abstract*— This paper presents a coverage control algorithm for teams of quadcopters with downward facing visual sensors that prevents the appearance of coverage holes in-between the monitored areas while maximizing the coverage quality as much as possible. We derive necessary and sufficient conditions for preventing the appearance of holes in-between the fields of views among trios of robots. Because this condition can be expressed as logically combined constraints, control nonsmooth barrier functions are implemented to enforce it. An algorithm which extends control nonsmooth barrier functions to hybrid systems is implemented to manage the switching among barrier functions caused by the changes of the robots composing trio. The performance and validity of the proposed algorithm are evaluated in simulation as well as on a team of quadcopters.**

I. Introduction

Visual sensor networks have been used in urban areas and natural environments [1], [2] with the intention of gathering information about events such as human activities [3], traffic flows [4], terrain data [5], and natural phenomena [6]. Aside from systems that employ fixed or directionally controllable cameras [7], [8], the use of aerial robot teams with visual sensors is rapidly emerging within environmental monitoring applications [9], [10]. However, when a team of aerial robots is required to monitor broad areas of interest or visually track targets [11], coverage holes may appear in-between the fields of view (FOVs) of the different robots. This can result in the team potentially overlooking important events—an undesirable operational feature of the system.

Cooperative environmental monitoring with multi-robot teams can be considered in the context of the coverage problem [12], [13], [14], [15], [16], which grants an optimal deployment of a group of mobile sensors over a domain in a distributed fashion. Several criteria can be taken into account when evaluating the coverage performance of the team, and the elimination of coverage holes constitutes an important aspect in the development of some approaches concerning coverage of areas over uniform importance densities [17], [18]. Regarding coverage control with visual sensor networks [19], [20], [21], [22], the quality of monitoring is often evaluated with respect to the spatial sensing quality of the visual sensor and the importance of the covered area.

In this paper, we consider a visual coverage control strategy which prevents the appearance of unmonitored areas in-between the FOVs of neighboring quadcopters—namely *coverage holes*—while maximizes the coverage quality as much as possible. While the elimination of coverage holes is not discussed in visual coverage control [21], [22], an algorithm reducing coverage holes in mobile sensors is presented in [17], which however does not guarantee the elimination of holes. In the author's previous work [23], this problem was addressed by incorporating control barrier functions (CBFs) to a visual coverage control algorithm to ensure coverage holes are not formed in-between monitored areas. However, the CBFs implemented in [23] only consider sufficient conditions for the formation of holes, hence rendering an excessively conservative controller. Furthermore, the CBFs in the previous approach cannot manage changes regarding which quadcopters should prevent the formation of a hole among them, which resulted in the team being forced to keep the graph generated based on the initial positions of the robots. Therefore, as the number of quadcopters in the team increases, the movement of the quadcopters executing the coverage algorithm in [23] becomes overly restrictive, which in turn significantly deteriorates the coverage quality.

This paper addresses these two issues: we eliminate the excessive conservativeness of the CBFs in [23] (while maintaining the prevention of holes) and allow the graph related to the elimination of holes among quadcopters to be dynamic. To this end, we derive necessary and sufficient conditions to not make any holes among any three agents with overlapping FOV areas. Because this condition entails Boolean logic, the proposed method utilizes control nonsmooth barrier functions (CNBFs), which support Boolean composition of CBFs. Then, we extend these newly designed CNBFs to large teams of quadcopters, where the Delaunay graph associated with the power diagram [24] (a weighted Voronoi diagram characterized by the radii of the agents' FOV) changes over time. To address the jumps in the values of the CNBFs caused by the switchings, the proposed algorithm extends the newly designed CNBFs to hybrid systems.

The paper is organized as follows. Section II introduces the problem formulation. The CNBF that prevents the appearance of holes between neighboring quadcopters is proposed

*This work was supported by JSPS KAKENHI Grant Number 18H01459, 18H05903 and by grant number DCIST CRA W911NF-17-2-0181 from the US Army Research Lab.

[1]R. Funada is with Department of Aerospace Engineering and Engineering Mechanics, The University of Texas at Austin, TX 78712, USA riku.funada@austin.utexas.edu

[2]M. Santos and M. Egerstedt are with the School of Electrical and Computer Engineering, Georgia Institute of Technology, Atlanta, GA 30332, USA {maria.santos,magnus}@gatech.edu

[3]T. Gencho, J. Yamauchi, and M. Fujita are with Department of Systems and Control Engineering, Tokyo Institute of Technology, Tokyo 152-8550, Japan {gencho,yamauchi,fujita}@sc.e.titech.ac.jp

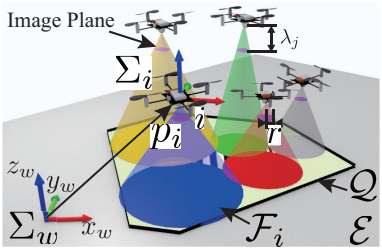

Fig. 1. Proposed scenario. The mission space $\mathcal{Q}$ on the environment $\mathcal{E}$ is monitored by a team of quadcopters. Quadcopter i has a circular field of view $\mathcal{F}_i$, which depends on its position p_i and focal length λ_i. The crosshatched area in-between the quadcopters' fields of view shows a hole.

in Section III, under the assumption of a static graph. Section IV reconsiders the proposed scenario as a hybrid system, and extends the result in Section III into large numbers of agents with the switching of the graph. The performance of the proposed algorithm is evaluated in simulation and experiments in Section V. Section VI concludes this paper.

II. Problem Formulation

In this paper, we consider the scenario illustrated in Fig. 1, where n quadcopters, labeled through the index set $\mathcal{N} = \{1, \cdots, n\}$, equipped with cameras are distributed over 3-D Euclidean space to monitor a planar region, which is denoted as the mission space $\mathcal{Q}$. The mission space is a closed and bounded convex subspace of the environment $\mathcal{E}$. A density function, $\phi : \mathcal{E} \to \mathbb{R}_+ := [0, \infty)$, encodes the importance of each point on $\mathcal{E}$ so that, the higher the importance, the higher the value of ϕ in $\mathcal{Q}$, with $\phi(q) = 0,\ q \in \mathcal{E} \backslash \mathcal{Q}$.

The world coordinate frame, Σ_w, is arranged so that its X_wY_w-plane is coplanar with $\mathcal{E}$ where the standard basis of Σ_w is described as $\{\mathbf{e}_x, \mathbf{e}_y, \mathbf{e}_z\}$. Then, the environment is described as $\mathcal{E} = \{q \in \mathbb{R}^3 \mid \mathbf{e}_z^T q = 0\}$, and the quadcopters are confined in the half space $\{q \in \mathbb{R}^3 \mid \mathbf{e}_z^T q > 0\}$.

Let Σ_i be the coordinate frame of Quadcopter $i \in \mathcal{N}$, located at $p_i = [x_i, y_i, z_i]^T$ with respect to Σ_w, and its attitude is fixed to coincide with that of Σ_w regardless of Quadcopter i's attitude. We assume that each quadcopter mounts a visual sensor with a gimbal which keeps its image plane always parallel to the X_iY_i-plane and Z_i aligned with the optical axis. If we utilize a perspective projection model [25] to express the image projection, the origin of Σ_i is located at a distance equal to the focal length, λ_i, above the image plane. In this paper, the image planes of all quadcopters are assumed to be circular with radius r.

The state of Quadcopter i is defined as $\mathbf{p}_i = [p_i^T, \lambda_i]^T$, where focal length λ_i decides the zoom level of its visual sensor. We suppose that the motion of the Quadcopter $i \in \mathcal{N}$ can be described according to single integrator dynamics,

$$\dot{\mathbf{p}}_i(t) = u_i(t),\ \mathbf{p}_i(t_0) = \mathbf{p}_{i0},\ t_0 \in \mathbb{R},\ t \in \mathbb{R}_{>t_0} \quad (1)$$

which can be converted to reflect the quadcopter's dynamics, e.g. as in [26]. Then, Quadcopter i can monitor the part of the environment $\mathcal{E}$ in its FOV

$$\mathcal{F}_i = \left\{ q \in \mathcal{E} \;\middle|\; \|q - [x_i, y_i, 0]^T\| \leq r\frac{z_i}{\lambda_i} \right\}.$$

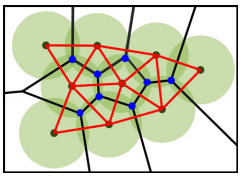

Fig. 2. Power diagram induced by 9 agents, depicted with black lines. The FOV of each agent and the graph $\mathcal{G}$ are illustrated by the green circles and the red lines, respectively. The vertices of the power diagram in-between agents, shown in blue dots, are generated by groups of three agents. On the left, the boundary of $\bigcup_{i=1}^n \mathcal{F}_i$ has a dent with a vertex generated by 3 agents, but this does not represent a hole according to Definition 1.

The quality of surveillance of a point $q \in \mathcal{F}_i$ can be modeled using the results from [19],

$$f(\mathbf{p}_i, q) = \frac{\sqrt{\lambda_i^2 + r^2}}{\sqrt{\lambda_i^2 + r^2} - \lambda_i} \left(\frac{z_i}{\|q - p_i\|} - \frac{\lambda_i}{\sqrt{\lambda_i^2 + r^2}} \right) \times \left(\frac{\lambda_i}{\sqrt{\lambda_i^2 + r^2}} \right)^{\kappa} \exp\left(-\frac{(\|q - p_i\| - R)^2}{2\sigma^2} \right), \quad (2)$$

where $\kappa, \sigma, R > 0$ model the characteristics of the visual sensor. If $q \in \mathcal{Q}$ is not in $\mathcal{F}_i$, then we set $f(\mathbf{p}_i, q) = 0$.

With the sensing performance function (2), the quality of coverage performed by the team of quadcopters, with their combined state denoted as $\mathbf{p} = [\mathbf{p}_1^T, \cdots, \mathbf{p}_n^T]^T$, as

$$\mathcal{H}(\mathbf{p}) = \int_{\mathcal{Q}} \max_{i \in \mathcal{N}} f(\mathbf{p}_i, q)\phi(q)\mathrm{d}q, \quad (3)$$

which is proposed as $\mathcal{H}_{\mathcal{C}}$ in the author's previous work [23]. Then, the nominal control input to maximize the coverage quality can be calculated in a distributed fashion as

$$u_{i,\mathrm{nom}} = \alpha \frac{\partial \mathcal{H}(\mathbf{p})^T}{\partial \mathbf{p}_i}, \quad i \in \mathcal{N}, \alpha \in \mathbb{R}_+. \quad (4)$$

We assume that each quadcopter is able to send its state to the neighboring agents, being the inter-agent communication modeled by the graphs $\mathcal{G}_{\mathcal{F}}(t)$ and $G_{\mathcal{P}}(t)$. First, let $\mathcal{G}_{\mathcal{F}}(t)$ denote the graph which has an edge between $i, j \in \mathcal{N}$ if Quadcopters i and j have overlapping FOVs, i.e. $\mathcal{F}_i \cap \mathcal{F}_j \neq \emptyset$. Second, $G_{\mathcal{P}}(t)$ is the graph determined by the power diagram [24], characterized by the weighted distance

$$d_{\mathcal{P}}(\mathbf{p}_i, q) = \|[q_x, q_y]^T - [x_i, y_i]^T\|^2 - \Delta_i^2, \quad (5)$$

where $\Delta_i = rz_i/\lambda_i$ is the radius of $\mathcal{F}_i$. Then, the communication graph is given by $\mathcal{G}(t) = \mathcal{G}_{\mathcal{F}}(t) \cap \mathcal{G}_{\mathcal{P}}(t)$, which preserves the edges of power diagram only between those neighbors whose FOVs overlap. We denote Quadcopter i's neighbors in graph $\mathcal{G}(t)$ as $\mathcal{N}_i(t)$. An example of a power diagram and associated $\mathcal{G}(t)$ is depicted in Fig. 2, where a boundary of power diagram between Agents i, j connected by an edge of $\mathcal{G}(t)$ is composed of the line passing through two intersection points of their FOVs.

The goal of this paper is to present the algorithm which prevents the formation of unsurveilled areas among the quadcopter's FOVs $\{\mathcal{F}_1, \cdots, \mathcal{F}_n\}$ while minimally changing the nominal input $u_{i,\mathrm{nom}}$ in (4). Similar to the disk-covering problem [27], this paper prevents the appearance of holes by

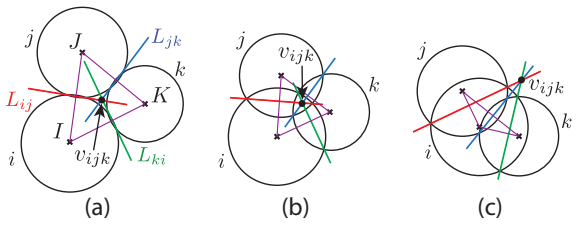

Fig. 3. Three cases of FOV deployments. (a) shows a hole in the sense of Def. 1, where v_{ijk} lies outside of all three FOVs. (b) and (c) do not have a hole, but v_{ijk} exists outside of FOVs in (c). This implies that the CBF in (7) restricts the configuration in (c) just like (a), even if (c) does not contain any holes. $\triangle IJK$ is depicted as a purple triangle in each subfigure.

including Voronoi vertices, which lie in-between FOVs of teams, in FOVs of quadcopters. Considering that all Voronoi vertices among teams' FOVs are formed by three agents, as shown in Fig. 2, except for degenerate Voronoi diagrams [28], we can divide the problem into triangular subgraphs of $\mathcal{G}(t)$. Note that, in practice, degenerate Voronoi diagrams do not cause severe problems since they can be separated into triangulations.

From the above observation, in Section III, we restrict our attention to the unsurveilled areas that may arise between any three agents determined by a triangular subgraph of $\mathcal{G}(t)$, assuming $\mathcal{G}(t)$ static. The derived condition for preventing the appearance of holes is described as the CNBF, which allows us to confine agents within the set determined by logically combined constraints. Then, the newly designed CNBF is extended to large teams where there appear switching in the CNBFs as a consequence of changes in the graph.

III. No-Hole Coverage with 3 Agents

In this section, we assume $n = 3$ to design the CNBF for preventing formation of holes, neglecting discontinuities in the constraints caused by the changes on the graph $\mathcal{G}(t)$. The proposed method will be extended to larger teams, $n > 3$, with (potentially) changing graphs $\mathcal{G}(t)$ in Section IV. Hereafter, we denote the point $I = [x_i, y_i, 0]$ as a horizontal position of Quadcopter i projected on the environment $\mathcal{E}$.

First, we formally define the concept of a *hole* as considered throughout the paper.

Definition 1: Let all pairs $\{i, j, k\}$ have an edge determined by the graph $\mathcal{G}$. Then, a closed set $E \subset \mathcal{Q}$ is said to be a *hole*, if and only if it satisfies the conditions

$$\begin{aligned}(\partial E \cap \partial \mathcal{Q} = \emptyset) \ \wedge \ (\mathrm{Int}(E) \cap \mathcal{F}_i = \emptyset, \ \forall i \in \mathcal{N}) \\ \wedge \ (E \subset \triangle IJK),\end{aligned} \tag{6}$$

where ∂E and $\partial \mathcal{Q}$ denote the boundaries of E and $\mathcal{Q}$; $\mathrm{Int}(E)$, the interior of E; and $\triangle IJK$, the triangle with vertices I, J, and K

Figure 3(a) shows a hole as defined in Def. 1 where the radical center $v_{ijk} = [v^x_{ijk}, v^y_{ijk}]^T$—a vertex of the cell of the power diagram—is the intersection of three radical axes L_{ij}, L_{jk}, and L_{ki}. Without loss of generality, we make the following assumption.

Assumption 1: No pair in $\{\partial\mathcal{F}_i, \partial\mathcal{F}_j, \partial\mathcal{F}_k\}$ contains sensing regions that are concentric. Also, not two axes among $\{L_{ij}, L_{jk}, L_{ki}\}$ are parallel.

Assumption 1 guarantees the radical axes $\{L_{ij}, L_{jk}, L_{ki}\}$ exist and intersect at a single point, and $\triangle IJK$ does not become a degenerate triangle.

We want to ensure that no hole appears among teams' FOVs during the coverage operation if the initial deployment of quadcopters does not present any holes. To this end, the authors' previous work [23] confined the state of Quadcopter i in the superlevel set $C_{i,\mathcal{F}} = \{\mathbf{p}_i \in \mathbb{R}^4 \mid h_{i,\mathcal{F}} > 0\}$ of a function $h_{i,\mathcal{F}}$, called a CBF [29],

$$h_{i,\mathcal{F}} = \left(r\frac{z_i}{\lambda_i}\right)^2 - \left((v^x_{ijk} - x_i)^2 + (v^y_{ijk} - y_i)^2\right), \tag{7}$$

where (7) is a slightly modified version of [23, Equation 24]. $C_{i,\mathcal{F}}$ is interpreted as the set in which $v_{ijk} \in \mathcal{F}_i$ is satisfied as illustrated in Fig. 3(b), and [23] proved that $h_{i,\mathcal{F}} > 0$ is the sufficient condition of not making a hole between Agents i, j, and k. However, as depicted in Fig. 3(c), the condition $h_{i,\mathcal{F}} > 0$ is so conservative that it affects certain movements between quadcopters, even if such movements do not incur the appearance of holes.

In order to relax this condition, let us consider the relationship between holes and $\triangle IJK$. From the difference between Fig. 3(a) and (c), where v_{ijk} is outside of $\mathcal{F}_i$ in both cases but a hole appears only in (a), the condition $v_{ijk} \in \triangle IJK$ seems to play an important role. In other words, to prevent the appearance of holes, Quadcopter i needs to satisfy $v_{ijk} \in \mathcal{F}_i$ only when $v_{ijk} \in \triangle IJK$ holds. This can be written as

$$\neg\left(v_{ijk} \in \triangle IJK\right) \vee \left(v_{ijk} \in \mathcal{F}_i\right). \tag{8}$$

The following Theorem formalizes the relationship between (8) and the existence of a hole.

Theorem 1: Let us consider Agents i, j, and k, where each agent's sensing region intersects with that of the other two agents. Then, there is no hole in-between the three agents if and only if the condition (8) is satisfied.

Proof: First, we prove the necessary condition by examining its contraposition

$$\left(v_{ijk} \in \triangle IJK\right) \wedge \left(v_{ijk} \notin \mathcal{F}_i\right) \Rightarrow E \neq \emptyset. \tag{9}$$

Given that each circle intersects the two other circles, each side of the triangle is contained in the set $(\mathcal{F}_i \cup \mathcal{F}_j \cup \mathcal{F}_k)$. This means that, if the triangle does not contain a hole ($E = \emptyset$), then $\triangle IJK \subset (\mathcal{F}_i \cup \mathcal{F}_j \cup \mathcal{F}_k)$ always holds. Based on the fact there are only two possibilities for the location of v_{ijk}: (i) v_{ijk} lies on or inside all three circles $\mathcal{F}_i \cap \mathcal{F}_j \cap \mathcal{F}_k$; or (ii) v_{ijk} lies outside of three circles $\mathcal{F}_i \cup \mathcal{F}_j \cup \mathcal{F}_k$ [30], the left side of the proposition (9) holds only if a hole exists. This proves the proposition (9).

Second, we prove the sufficient condition

$$\neg\left(v_{ijk} \in \triangle IJK\right) \vee \left(v_{ijk} \in \mathcal{F}_i\right) \Rightarrow E = \emptyset. \tag{10}$$

In [23, Lemma 2], the statement $(v_{ijk} \in \mathcal{F}_i) \Rightarrow E = \emptyset$ was proved. Therefore, we only show that

$$\neg\left(v_{ijk} \in \triangle IJK\right) \Rightarrow E = \emptyset. \tag{11}$$

If we consider the case of $E \neq \emptyset$, $\mathcal{F}_i \cap \mathcal{F}_j \cap \mathcal{F}_k = \emptyset$ is satisfied. Because the location of v_{ijk} is limited to case (i) or (ii) as stated in the proof of the necessary condition, the possible location of v_{ijk} under the condition of $E \neq \emptyset$ is only (ii) outside of all three circles $\mathcal{F}_i \cup \mathcal{F}_j \cup \mathcal{F}_k$. Considering this with the characteristics of v_{ijk} as the power center, $E \neq \emptyset \Rightarrow v_{ijk} \in E \subset \triangle IJK$ is satisfied. This is the contraposition of the statement (11), thus a sufficient condition is proved. ■

The statement $v_{ijk} \in \triangle IJK$ can be expressed as

$$(h_{IJK} > 0) \wedge (h_{JKI} > 0) \wedge (h_{KIJ} > 0), \tag{12}$$

where

$$h_{IJK} = \left(\mathbf{e}_z^T \left(\overrightarrow{IJ} \times \overrightarrow{Iv_{ijk}}\right)\right) \Big/ \left(\mathbf{e}_z^T \left(\overrightarrow{IJ} \times \overrightarrow{IK}\right)\right) > 0 \tag{13}$$

is a candidate CBF which takes a positive value when v_{ijk} and K are in the same half-plane divided by line IJ. Note that the denominator of (13) is not 0 if Assumption 1 is satisfied. Combining $h_{i,\mathcal{F}}$ with (12), (8) can be rewritten as

$$\neg\left((h_{IJK} > 0) \wedge (h_{JKI} > 0) \wedge (h_{KIJ} > 0)\right) \vee (h_{i,\mathcal{F}} > 0). \tag{14}$$

To prevent a hole appearance between FOVs of quadcopters, the state of Quadcopter $i \in \mathcal{N}$ must be confined in the set determined by (14), which is encoded by the Boolean composition of CBFs. The results of [31] reveal that a full system of Boolean logic with $\wedge, \vee$, and $\neg$ can be formed as

$$\begin{aligned} h_1 \wedge h_2 &:= \min\{h_1, h_2\},\ h_1 \vee h_2 := \max\{h_1, h_2\}, \\ \neg h_1 &:= -h_1. \end{aligned} \tag{15}$$

Therefore, (14) can be expressed as

$$h_i = \max\{-h_{IJK}, -h_{JKI}, -h_{KIJ}, h_{i,\mathcal{F}}\} > 0. \tag{16}$$

The CNBF (16) describes sufficient and necessary conditions (8) for preventing the appearance of holes between three neighboring agents. Hence, (16) successfully eliminates the conservativeness in the CBF in [23, Equation 24]. In next section, we introduce the tools which keep the state of Quadcopter i in the set (16) when the graph changes.

IV. No-Hole Coverage for Large Teams

In this section, we consider the control algorithm which prevents the appearance of holes among FOVs of teams with large numbers of quadcopters. As the number of quadcopters increases, it is more likely for $\mathcal{G}(t)$ to be dynamic. Accordingly, the CNBF (16), which Quadcopter i needs to evaluate in each triangular subgraph, may become discontinuous. This requires introducing tools that deal with hybrid systems [32].

First, let us introduce the following two definitions from [32], which are required to redefine the problem we consider.

Definition 2: [32, Def. 1] A sequence $\{\tau_k\}_{k=1}^{\infty}$ is a switching sequence for (1) if and only if it is strictly increasing, unbounded, and $\tau_1 = t_0$. With respect to $\{\tau_k\}_{k=1}^{\infty}$, let

$$K_{t_1} = \inf\left\{K \in \mathbb{N} \mid [t_0, t_1] \subset \bigcup_{k=1}^{K} [\tau_k, \tau_{k+1})\right\}. \tag{17}$$

Definition 3: [32, Def. 2] A set $\mathcal{D} \subset \mathbb{R}^n \times \mathbb{R}$ is hybrid forward invariant with respect to (1) and a switching sequence $\{\tau_k\}_{k=1}^{\infty}$ for (1) if and only if for every Carathéodry solution starting from x_0 at t_0,

$$(x(\tau_k), \tau_k) \in D, \forall k \leq K_{t_1} \Rightarrow (x(t), t) \in D, \forall t \in [t_0, t_1].$$

Along the lines of the aforementioned definitions, we first model the changes in the graph and constraints. We assume that the set of the triangular subgraph $\mathcal{T}_i(t)$ of the graph $\mathcal{G}(t)$, which contains Quadcopter i as its vertex, remains fixed over intervals indicated by a switching sequence $\{\tau_k\}_{k=1}^{\infty}$. Def. 3 expresses the behavior of the system pursuing in this paper. In the proposed scenario, it implies if the changes of the graph $\mathcal{G}(t)$ make no holes instantaneously in-between $\mathcal{T}_i(t), \forall i \in \mathcal{N}$, no holes appear among FOVs of teams. Note that the rigorous treatment of hybrid systems requires theories introduced in [33], but in this paper we omit to introduce those theories, because those operations are not required in the implementation of the proposed algorithm.

Then, the CNBF representing the constraint that Quadcopter i should not make a hole in-between each triangular subgraph $m_i \in \mathcal{T}_i(t)$ on the k-th interval is written as

$$\begin{aligned} h_{i,m_i}^k(\mathbf{p}_i, \mathbf{p}_j, \mathbf{p}_k) &= \max_{\ell}\{h_{m_i,\ell}^k\}, \\ \ell &= 1, \cdots, 4, m_i \in \mathcal{T}_i(\tau_k), \end{aligned} \tag{18}$$

by following (7), (12), and (16). Here, we define $h_{m_i,\ell}^k, (\ell = 1, \cdots, 4)$ for each of these triangular subgraph $m_i \in \mathcal{T}_i(\tau_k)$, where they correspond to $-h_{IJK}, -h_{JKI}, -h_{KIJ}$, and $h_{i,\mathcal{F}}$ in order when the vertices of m_i is i, j, and k for simplicity. By combining $h_{i,m_i}^k, \forall m_i \in \mathcal{T}_i(\tau_k)$ together, we obtain

$$h_i^k(\mathbf{p}_i, \mathbf{p}_{l\in\mathcal{N}_i}) = \bigwedge_{m_i=1}^{|\mathcal{T}_i(\tau_k)|} h_{i,m_i}^k, \tag{19}$$

which encapsulates the constraint that Quadcopter i must prevent the formation of holes in-between all neighboring agents $l \in \mathcal{N}_i$. (19) can be rewritten, by using (15), as

$$h_i^k(\mathbf{p}_i, \mathbf{p}_{l\in\mathcal{N}_i}) = \min_{m_i}\{h_{i,m_i}^k(\mathbf{p}_i, \mathbf{p}_j, \mathbf{p}_k)\}. \tag{20}$$

Hence, the goal of this paper can be translated as the proposal of algorithm which makes the set

$$C_i = \{(\mathbf{p}_i, t) \in \mathbb{R}^4 \times \mathbb{R}_{\geq t_0} \mid h_i(\mathbf{p}_i, \mathbf{p}_{l\in\mathcal{N}_i}, t) \geq 0\} \tag{21}$$

hybrid forward invariance, where

$$\begin{aligned} h_i(\mathbf{p}_i, \mathbf{p}_{l\in\mathcal{N}_i}, t) &= h_i^k(\mathbf{p}_i, \mathbf{p}_{l\in\mathcal{N}_i}), \\ &\forall k \in \mathbb{N}, \forall t \in [\tau_k, \tau_{k+1}), \forall \mathbf{p}_i \in \mathbb{R}^4 \end{aligned} \tag{22}$$

for Quadcopter $i \in \mathcal{N}$. (22) takes the similar form with a candidate control hybrid nonsmooth barrier function in [32]. However, (22) has a nested structure of logic composition. In other words, the max operator in (18) is nested by the min operator (20). Therefore, strictly speaking, in order to ensure hybrid forward invariance of the set C_i, we need an extension results of [31], [32]. In this paper, we focus on the proposal of algorithm which prevents the hole's

appearance and confirm its effectiveness through simulations and experiments.

The hybrid forward invariance of the set C_i can be achieved by guaranteeing

$$\dot{h}_i(\mathbf{p}_i, \mathbf{p}_{l\in\mathcal{N}_i}, t) \geq -\alpha(h_i(\mathbf{p}_i, \mathbf{p}_{l\in\mathcal{N}_i}, t)), a.e.[t_0, t_1] \ni t,$$

for every Carathéodry solution, for some locally Lipschtz extended class-$\mathcal{K}$ function $\alpha : \mathbb{R} \to \mathbb{R}$ [32]. However, the nonsmoothness exists in (18) and (20) prohibits calculating $\dot{h}_i$ via the usual chain rule. To address this issue, we introduce the almost-active set of functions,

$$I_{\epsilon,i}(x', t') = \{i \mid \|h_i(x', t') - h(x', t')\| \leq \epsilon\}, \tag{23}$$

and the almost-active gradient

$$\partial_\epsilon h(x', t') = \text{co} \bigcup_{i\in I_{\epsilon,i}(x',t')} \partial h_i(x', t'), \tag{24}$$

at $(x', t') \in \mathbb{R}^n \times \mathbb{R}_{\geq 0}$ [32].

For a CNBF composed by continuously differentiable functions, [31] shows that utilizing the almost-active gradient as a constraint in a quadratic programming (QP) generates the control input satisfying constraints, with assuming the resulting controller is measurable and locally bounded. The work in [32], which considers switching constraints in hybrid systems, also takes this approach with putting the gradients of the component functions in constraints, while eliminating the convex-hull operation in (24). Since the individual gradients of the component function in (7) and (12) at each point in time is smooth under Assumption 1 and they are combined by operators in (15), we also follow the approach proposed in [31] to make the set C_i hybrid forward invariance.

Given $u_{i,\text{nom}}$ in (4), the QP minimally modifying $u_{i,\text{nom}}$ to prevent the appearance of holes on each interval can be described as

$$\begin{aligned} u_i^* = &\arg\min_{u_i\in\mathbb{R}^4} (u_i - u_{i,\text{nom}})^T W (u_i - u_{i,\text{nom}}) \\ \text{s.t. } &\frac{\partial h^k_{m_i,\ell}(\mathbf{p}_i, \mathbf{p}_{j\in\mathcal{N}_i})}{\partial \mathbf{p}_i}^T u_i \geq -\gamma h_i^k(\mathbf{p}_i, \mathbf{p}_{j\in\mathcal{N}_i})^3, \\ &\forall m_i \in I^k_{\epsilon,m_i}(\mathbf{p}_i, \mathbf{p}_{j\in\mathcal{N}_i}),\ \forall \ell \in I^k_{\epsilon,\ell}(\mathbf{p}_i, \mathbf{p}_{j\in\mathcal{N}_i}), \end{aligned} \tag{25}$$

with $W = \text{diag}(1, 1, 1, w_\lambda)$ under the following assumption.

Assumption 2: From the perspective of Quadcopter i, the neighboring Quadcopters $j \in \mathcal{N}_i$ do not move.

Here, w_λ is introduced to adjust the unit difference between p_i and λ_i. Assumption 2 implies Quadcopter i need not calculate $\frac{\partial h^k_{m_i,\ell}}{\partial \mathbf{p}_j}, j \in \mathcal{N}_i$, when solving the QP in a distributed manner. Although in reality Quadcopters $j \in \mathcal{N}_i$ are indeed moving, they are also preventing to make a hole between them and Quadcopter i, and their speed is low. Thus, we can assume Quadcopters $j \in \mathcal{N}_i$ are not moving with respect to i. The entire process is shown in Alg. 1.

Algorithm 1 achieves the hybrid forward invariance of the set C_i in the sense of Def. 3, which does not consider holes suddenly generated by the changes in the graph $\mathcal{G}(t)$. However, in the proposed scenario, there are some cases where switches in the graph may cause the sudden appearance of a hole. As shown in the left part of Fig. 2, the boundary of $\bigcup_{i=1}^n \mathcal{F}_i$ can have a dent. If one of the quadcopters approaches and attaches itself to this dent, the graph $\mathcal{G}(t)$ may change and this dent may turn into a hole. Note that this hole's appearance does not break hybrid forward invariance of the set C_i in the sense of Def. 3. In addition, Alg. 1 eliminates this suddenly appeared hole in most cases, due to the robustness of the forward invariance of C_i. This phenomenon is illustrated in Fig. 6 for $k = 744$ and will further be explained in Section V.

Algorithm 1 Coverage maintenance algorithm

INPUT: Nominal controller: $u_{i,\text{nom}}$
The set of current triangular subgraph for i: $\mathcal{T}_i(\tau_k)$
OUTPUT: Coverage maintenance controller: u_i^*
$h^k_{i,m_i}(\mathbf{p}_i, \mathbf{p}_j, \mathbf{p}_k) \leftarrow \max_\ell\{h^k_{m_i,\ell}\}$,
$\ell = 1, \cdots, 4,\ \forall m_i \in \mathcal{T}_i(\tau_k)$
$h_i^k(\mathbf{p}_i, \mathbf{p}_{j\in\mathcal{N}_i}) \leftarrow \min_{m_i}\{h^k_{i,m_i}(\mathbf{p}_i, \mathbf{p}_j, \mathbf{p}_k)\}$
$I^k_{\epsilon,m_i} \leftarrow \emptyset$, $I^k_{\epsilon,\ell} \leftarrow \emptyset$
for $m_i = 1 : |\mathcal{T}_i(\tau_k)|$ **do**
  if $\|h^k_{i,m_i} - h_i^k\| \leq \epsilon$ **then**
    $I^k_{\epsilon,m_i}(\mathbf{p}_i, \mathbf{p}_{j\in\mathcal{N}_i}) \cup \{m_i\}$
    for $\ell = 1 : 4$ **do**
      if $\|h^k_{m_i,\ell} - h^k_{i,m_i}\| \leq \epsilon$ **then**
        $I^k_{\epsilon,\ell}(\mathbf{p}_i, \mathbf{p}_{j\in\mathcal{N}_i}) \cup \{\ell\}$
$u_i^* \leftarrow \arg\min_{u_i}(u_i - u_{i,\text{nom}})^T W (u_i - u_{i,\text{nom}})$
s.t. $\frac{\partial h^k_{m_i,\ell}(\mathbf{p}_i, \mathbf{p}_{j\in\mathcal{N}_i})}{\partial \mathbf{p}_i}^T u_i \geq -\gamma h_i^k(\mathbf{p}_i, \mathbf{p}_{j\in\mathcal{N}_i})^3$
$\forall m_i \in I^k_{\epsilon,m_i}(\mathbf{p}_i, \mathbf{p}_{j\in\mathcal{N}_i}),\quad \forall \ell \in I^k_{\epsilon,\ell}(\mathbf{p}_i, \mathbf{p}_{j\in\mathcal{N}_i})$

V. Simulations and Experiments

The proposed algorithm is implemented in simulation and experiment to verify that it renders the set C_i hybrid forward invariant. For both the simulation and experiment, the density function is shown as contour maps in snapshots.

First, Alg. 1 is compared with the nominal input in (4) (i.e. without hole prevention) and with the CBF from [23], in a simulation with 9 quadcopters. The size of mission space is $55 \times 55\,\text{m}^2$ as shown in Fig. 4. The parameters are set as $\kappa = 4, \sigma = 3, R = 11, w_\lambda = 3 \times 10^6$. The snapshots of the simulations for three methods are presented in Fig. 4. Figure 4(a) shows the transient state of quadcopters only with $u_{i,\text{nom}}$, and a hole appears in-between FOVs, which is undesirable. Fig. 4(b) and 4(c) show the final state of $u_{i,\text{nom}}$ with the CBF from [23] and Alg. 1, respectively. Both simulations do not exhibit holes. However, the CBF in [23] cannot change its graph, depicted in the red lines, from its initial state. This restricts quadcopters movement excessively. Figure 5 also supports this observation, where $u_{i,\text{nom}}$ modified by CBF in [23] cannot reach the coverage performance of Alg. 1 or $u_{i,\text{nom}}$. $h_i^k(\mathbf{p}_i, \mathbf{p}_{j\in\mathcal{N}_i}), \forall i \in \mathcal{N}$ of Alg. 1 is drawn in Fig. 6, where it takes the positive value except for $k = 744$. As explained in the end of Section IV, this is caused by the sudden appearance of a hole, and does not violate the hybrid forward invariance of the set.

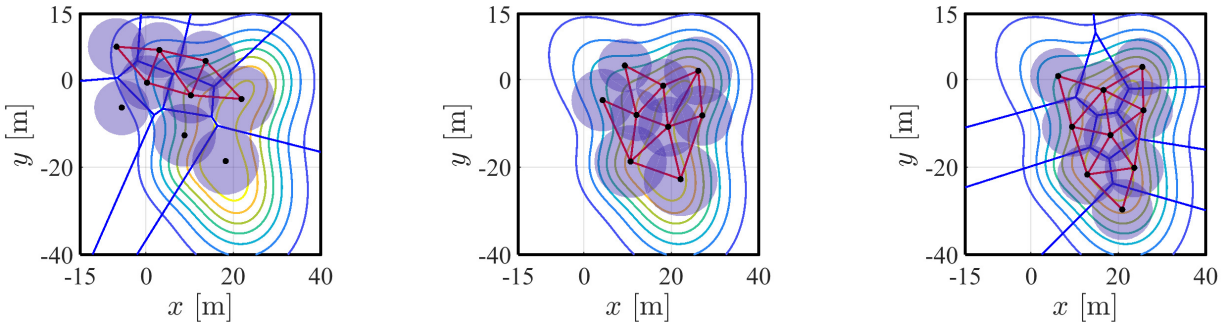

(a) Transient state using the nominal input in (4). (b) Final state with the CBF from [23]. (c) Final state executing the proposed algorithm.

Fig. 4. Snapshots of the simulations, where graph $\mathcal{G}$, dynamic in (a) and (c) and static in (b), is depicted in red. In transient state, a hole arises in (a) towards the center of the field, which takes time to eliminate. The methods in (b) and (c) prevent the hole's appearance during operation, but the static graph in (b) excessively restricts the quadcopters' movements. As a result, the FOVs in (b) are bigger and present larger overlaps than those in (c).

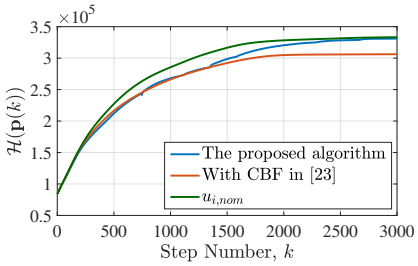

Fig. 5. Evolution of the cost function (3). Alg. 1 achieves a coverage quality as high as the nominal input, while [23] attains a suboptimal value.

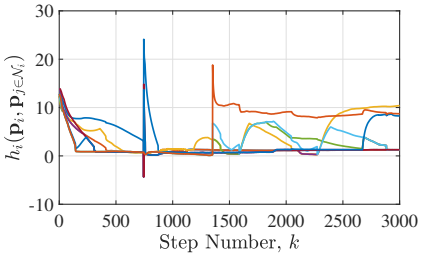

Fig. 6. Evolution of $h_i(\mathbf{p}_i, \mathbf{p}_{j\in\mathcal{N}_i}), \forall i \in \mathcal{N}$ in (22). Alg. 1 remains h_i in the positive value except for step number $k = 744$, at which a newly appeared triangular subgraph of $\mathcal{G}$ creates a hole as explained in the end of Section IV. Note that this instantaneously appeared hole does not violate the hybrid forward invariance of the set C_i in the sense of Def. 3.

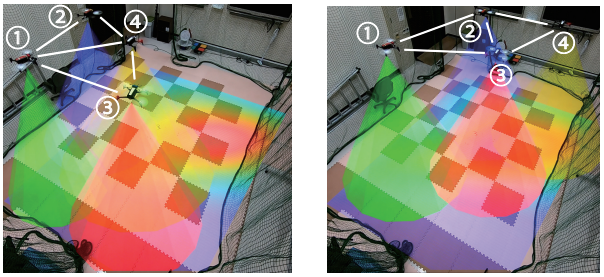

(a) (b)

Fig. 7. Snapshots of the experiment. (a): Initial condition. (b): Final condition. The density function overlaid on the floor takes higher value on the upper-right corner. FOVs of teams are drawn in the green, blue, red, and yellow cones. The indices and the graph $\mathcal{G}$ are shown in white.

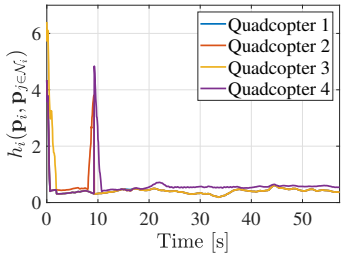

Fig. 8. $h_i(\mathbf{p}_i, \mathbf{p}_{j\in\mathcal{N}_i}), \forall i \in \mathcal{N}$ during the experiment. All value remains in the positive value, hence the appearance of hole is successfully prevented by Alg. 1. A spike at $t = 10\,\mathrm{s}$ is caused by the change of the graph.

Second, the proposed algorithm was implemented on a team of 4 quadcopters PARROT BEBOP 2. The size of experimental field is $4.2 \times 3.0\,\mathrm{m}^2$. We set their FOVs virtually. The parameters are set as $\kappa = 4, \sigma = 0.25, R = 2.2, w_\lambda = 6 \times 10^6$. As shown in Fig. 7, teams starting from the lower-left corner reach high density areas. $h_i(\mathbf{p}_i, \mathbf{p}_{j\in\mathcal{N}_i}), \forall i \in \mathcal{N}$ during the experiment are depicted in Fig. 8, where it can be observed that they remain positive throughout the experiment. Therefore, the proposed algorithm successfully modifies the nominal input in a minimally invasive way ensuring that no holes appear in-between the team's FOVs.

VI. Conclusion

This paper presented a visual coverage algorithm which prevents the formation of unsurveyed areas in-between fields of views of robots. Necessary and sufficient conditions for preventing the appearance of holes among trios of robots were derived. A new control nonsmooth barrier function was incorporated into the proposed algorithm to extend the results to teams composed of larger numbers of robots, where the topology is dynamic. The effectiveness of the proposed algorithm was demonstrated through simulation and experiment.

VII. Acknowledgement

The authors wish to acknowledge Dr. Paul Glotfelter for his help in interpreting the contents in Section IV.

REFERENCES

[1] X. Wang, "Intelligent multi-camera video surveillance: A review," *Pattern Recognition Letters*, vol. 34, no. 1, pp. 3–19, 2013.

[2] B. Rinner and W. Wolf, "An introduction to distributed smart cameras," *Proceedings of the IEEE*, vol. 96, no. 10, pp. 1565–1575, 2008.

[3] S. Fleck and W. Strasser, "Smart camera based monitoring system and its application to assisted living," *Proceedings of the IEEE*, vol. 96, no. 10, pp. 1698–1714, 2008.

[4] H. Zhou, H. Kong, L. Wei, D. Creighton, and S. Nahavandi, "Efficient road detection and tracking for unmanned aerial vehicle," *IEEE Transactions on Intelligent Transportation Systems*, vol. 16, no. 1, pp. 297–309, 2015.

[5] D. T. Cole, A. H. Goktogan, P. Thompson, and S. Sukkarieh, "Mapping and tracking," *IEEE Robotics Automation Magazine*, vol. 16, no. 2, pp. 22–34, 2009.

[6] G. Zhou, C. Li, and P. Cheng, "Unmanned aerial vehicle (UAV) real-time video registration for forest fire monitoring," in *Proceedings of 2005 IEEE International Geoscience and Remote Sensing Symposium*, vol. 3, 2005, pp. 1803–1806.

[7] S. Zhang, G. Wu, J. P. Costeira, and J. M. F. Moura, "Understanding traffic density from large-scale web camera data," in *Proceedings of 2017 IEEE Conference on Computer Vision and Pattern Recognition*, 2017, pp. 4264–4273.

[8] A. A. Morye, E. Franco, A. K. Roy-Chowdhury, and J. A. Farrell, "Distributed camera control via moving horizon bayesian optimization," in *Proceedings of 2014 American Control Conference*, 2014, pp. 2083–2089.

[9] H. Shakhatreh, A. H. Sawalmeh, A. Al-Fuqaha, Z. Dou, E. Almaita, I. Khalil, N. S. Othman, A. Khreishah, and M. Guizani, "Unmanned aerial vehicles (UAVs): A survey on civil applications and key research challenges," *IEEE Access*, vol. 7, pp. 48 572–48 634, 2019.

[10] S. Chung, A. A. Paranjape, P. Dames, S. Shen, and V. Kumar, "A survey on aerial swarm robotics," *IEEE Transactions on Robotics*, vol. 34, no. 4, pp. 837–855, 2018.

[11] T. Hatanaka, N. Chopra, M. Fujita, and M. Spong, *Passivity-Based Control and Estimation in Networked Robotics*. Springer-Verlag, 2015.

[12] J. Cortes, S. Martinez, T. Karatas, and F. Bullo, "Coverage control for mobile sensing networks," *IEEE Transactions on Robotics and Automation*, vol. 20, no. 2, pp. 243–255, 2004.

[13] C. G. Cassandras and W. Li, "Sensor networks and cooperative control," *European Journal of Control*, vol. 11, no. 4, pp. 436–463, 2005.

[14] S. Martinez, J. Cortes, and F. Bullo, "Motion coordination with distributed information," *IEEE Control Systems Magazine*, vol. 27, no. 4, pp. 75–88, 2007.

[15] M. Santos, S. Mayya, G. Notomista, and M. Egerstedt, "Decentralized minimum-energy coverage control for time-varying density functions," in *2019 International Symposium on Multi-Robot and Multi-Agent Systems (MRS)*, 2019, pp. 155–161.

[16] M. Santos, Y. Diaz-Mercado, and M. Egerstedt, "Coverage control for multirobot teams with heterogeneous sensing capabilities," *IEEE Robotics and Automation Letters*, vol. 3, no. 2, pp. 919–925, 2018.

[17] H. Mahboubi, K. Moezzi, A. G. Aghdam, and K. Sayrafian-Pour, "Distributed deployment algorithms for efficient coverage in a network of mobile sensors with nonidentical sensing capabilities," *IEEE Transactions on Vehicular Technology*, vol. 63, no. 8, pp. 3998–4016, 2014.

[18] B. Khalifa, Z. Al Aghbari, A. M. Khedr, and J. H. Abawajy, "Coverage hole repair in WSNs using cascaded neighbor intervention," *IEEE Sensors Journal*, vol. 17, no. 21, pp. 7209–7216, 2017.

[19] O. Arslan, H. Min, and D. E. Koditschek, "Voronoi-based coverage control of Pan/Tilt/Zoom camera networks," in *Proceedings of 2018 IEEE International Conference on Robotics and Automation*, 2018, pp. 1–8.

[20] M. Forstenhaeusler, R. Funada, T. Hatanaka, and M. Fujita, "Experimental study of gradient-based visual coverage control on SO(3) toward moving object/human monitoring," in *Proceedings of 2015 American Control Conference*, 2015, pp. 2125–2130.

[21] M. Schwager, B. J. Julian, M. Angermann, and D. Rus, "Eyes in the sky: Decentralized control for the deployment of robotic camera networks," *Proceedings of the IEEE*, vol. 99, no. 9, pp. 1541–1561, 2011.

[22] S. Papatheodorou, A. Tzes, and Y. Stergiopoulos, "Collaborative visual area coverage," *Robotics and Autonomous Systems*, vol. 92, pp. 126–138, 2017.

[23] R. Funada, M. Santos, J. Yamauchi, T. Hatanaka, M. Fujita, and M. Egerstedt, "Visual coverage control for teams of quadcopters via control barrier functions," in *Proceedings of 2019 International Conference on Robotics and Automation*, 2019, pp. 3010–3016.

[24] F. Aurenhammer, "Power diagrams: Properties, algorithms and applications," *SIAM Journal on Computing*, vol. 16, no. 1, pp. 78–96, 1987.

[25] Y. Ma, S. Soatto, J. Kosecka, and S. Sastry, *An Invitation to 3-D Vision: From Images to Geometric Models*. Springer-Verlag, 2003.

[26] D. Mellinger and V. Kumar, "Minimum snap trajectory generation and control for quadrotors," in *Proceedings of 2011 IEEE International Conference on Robotics and Automation*, 2011, pp. 2520–2525.

[27] J. Cortes and F. Bullo, "Coordination and geometric optimization via distributed dynamical systems," *SIAM Journal on Control and Optimization*, vol. 44, no. 5, pp. 1543–1574, 2005.

[28] A. Okabe, B. Boots, K. Sugihara, and S. N. Chiu, *Spatial Tessellations: Concepts and Applications of Voronoi Diagrams, Second Edition*. Wiley-Blackwell, May 2000.

[29] A. D. Ames, X. Xu, J. W. Grizzle, and P. Tabuada, "Control barrier function based quadratic programs for safety critical systems," *IEEE Transactions on Automatic Control*, vol. 62, no. 8, pp. 3861–3876, 2017.

[30] C. I. Delman and G. Galperin, "A tale of three circles," *Mathematics Magazine*, vol. 76, pp. 15–32, 2003.

[31] P. Glotfelter, J. Cortés, and M. Egerstedt, "Boolean composability of constraints and control synthesis for multi-robot systems via nonsmooth control barrier functions," in *Proceedings of 2018 IEEE Conference on Control Technology and Applications*, 2018, pp. 897–902.

[32] P. Glotfelter, I. Buckley, and M. Egerstedt, "Hybrid nonsmooth barrier functions with applications to provably safe and composable collision avoidance for robotic systems," *IEEE Robotics and Automation Letters*, vol. 4, no. 2, pp. 1303–1310, 2019.

[33] J. Cortes, "Discontinuous dynamical systems," *IEEE Control Systems Magazine*, vol. 28, no. 3, pp. 36–73, 2008.